A study on corrosion products and processes of patinated tin bronze in formic acid

Ying Yan[1] · Cong Zou[1] · Lehua Zhang[1,3] · Yan Zhu[1] · Laiming Wu[2] · Hao Zhou[2] · Lankun Cai[1]

Abstract

The corrosion processes of bare bronze and three types of patina-bearing tin bronze in the presence of formic acid have been explored through laboratory exposure. Following exposure time of 4, 14 and 28 days, the morphology and composition of the corrosion products on the sample were characterized to investigate their evolution by using SEM, XRD and Raman. The results indicated that Cu_2O was first generated on the bare bronze surface, then $Cu(OH)_2$ was formed at the early stage of the corrosion and as the exposure time increased, $Cu(OH)(HCOO)$ and $Cu(HCOO)_2$ were further generated. Bronze with Cu_2O layer was destroyed by formic acid and converted into $Cu(HCOO)_2$, which was similar to the conversion process of corrosion products of bare bronze, except that, the account of products of bronze patinated with Cu_2O was more than that of bare bronze, indicating that the Cu_2O layer on the sample surface was destroyed and further transformed. The main corrosion product of bronze with CuCl patina was $Cu_2(OH)_3Cl$, which was consistent with the reaction process of powdery rust. For bronze with mixed patina, two corrosion processes of Cu_2O patina and CuCl patina proceed at the same time, and the corrosion products were $Cu(HCOO)_2$ and $Cu_2(OH)_3Cl$, which were basically consistent with the corrosion behavior of bronze covered with a Cu_2O and a CuCl patina.

✉ Hao Zhou
haoshm1970@163.com

✉ Lankun Cai
cailankun@126.com

1 State Environmental Protection Key Laboratory of Environmental Risk Assessment and Control on Chemical Process, College of Resources and Environmental Engineering, East China University of Science and Technology, Shanghai 200237, People's Republic of China

2 Shanghai Museum, Shanghai 200050, People's Republic of China

3 Shanghai Institute of Pollution Control and Ecological Security, Shanghai 200237, People's Republic of China

Introduction

Atmospheric corrosion is prone to lead to the metal deterioration in various environments, which is the overall result of several physicochemical reactions between metals and their surrounding environment. Atmospheric corrosion behavior of metals and alloys has been mainly investigated in the presence of gases such as carbon dioxide, sulfur dioxide, sulfuric acid, hydrochloric acid and organic acids. [1–4]. It was in recent years that organic acid corrosion has received extensive attention due to its great threat to the safety of metals [5–9]. It has been shown that organic acids, especially formic and acetic acids, play an important role in the atmospheric corrosion of metal [10–12].

Organic acids are one of the most important chemical classes used in several industries. These acids are not only used as reagents for the manufacture of various chemicals, but also can be produced in some industrial processes. And in a museum environment, organic acids can be used as cleaning reagents to remove harmful patinas or salts for the protection of artistic objects. But these acids are the main cause of destruction of museum objects as the concentration accumulates [13]. Various organic acids can be also found in the oil production, accelerating the localized corrosion of metals owing to the decrease in pH [6]. Moreover, certain organic acid vapors are known to corrode metals during storage and transportation when metals act as packages or containers [14]. Among all organic acids, formic and acetic acids are the most aggressive acids [6, 15, 16] and are the most common in the atmosphere [17]. In particular, high concentrations of formic and acetic acids are known to emit from all natural woods. Metals and their alloys appear to be susceptible to attack when they are exposed to the environment containing woods [5]. Besides that, a large amount of acetic acid was produced in the anodic polarization process of the titanium/ethanol system with the rapid decrease in pH, causing the stress corrosion of metals [18]. After exposing to the humid environment in the presence of formic or acetic acid for a long time, metals and their alloys suffered from serious damage, which will greatly affect their performance. Formic and acetic acids were reported to accelerate the corrosion of metals or alloys such as lead [7, 19, 20], bronze [9], copper [9, 14, 15, 17, 21] and steel [6, 8, 11, 22].

Preliminary exploration of the corrosion regulars of formic and acetic acids to metals has been carried out on various environmental conditions including temperature, pressure, humidity and concentration. A significant elevation of corrosion rates of mild steel with increasing acetic acid concentrations at high pressure and temperature was reported, which was justified by Okafor et al. [23], and the increased corrosion rates were thought to be associated with the reduction in adsorbed undissociated acetic acid on metal surfaces. Niklasson et al. [19, 20] found that formic and acetic acids strongly accelerate lead corrosion at 22.0 °C and 95% RH, and they suggested that the corrosion process of lead was enhanced because of the decreased pH in the surface electrolyte. Although most authors stated that formic and acetic acids increased corrosion rates at all studied conditions, some other researchers have found that acetic acid could act as an inhibitor

under certain conditions. Kahyarian et al. [8] reported that the acetic acid ranging from pH 3 to pH 5 inhibits corrosion with the concentrations up to 41.5 mmol when studying the aqueous mild steel corrosion in the presence of acetic acid, and George and Nesic [24] also found the corrosion of mild steel would be inhibited with increasing acetic acid concentration at room temperature. These results of nonuniform statements demand a detailed interpretation by further research on the mechanisms and regulars of metal corrosion related to formic and acetic acids.

The aim of the study is to investigate the corrosion behavior of tin bronze in the presence of formic acid. Bronze, as a metal widely used in various applications, such as industrial equipment, electricity, ornamental parts, [25], may come in contact with formic and acetic acids in oil and gas industries [23] or the indoor environment containing woods. Formic and acetic acids emitting from woods have been reported to be one of the main causes of bronze corrosion [5]. The common corrosion type of tin bronze includes uniform corrosion, localized corrosion, etc. Uniform corrosion proceeds over the entire exposed surface by a chemical or electrochemical reaction, while localized corrosion often occurs within crevices on the metal surface [25]. What's more, the patinas called bronze protective film would become unstable under acidic conditions [26], which also make the corrosion behavior of bronze different and more complicated in contrast to other metals. Nowadays, many scholars have studied the effect of formic acid or acetic acid on lead, copper, steel, etc. [6–9, 19–22]; there are also a few studies that report the corrosion of bronze by organic acids [9], but their role on patinated bronze is very scarcely available.

Hence, the corrosion behavior of patina-attached tin bronze in the presence of formic acid was investigated in this work, in order to explore the destruction mechanism of bronze and its patinas. Different analysis techniques were conducted to elucidate the morphology and composition of the corrosion product at different stages in the presence of formic acid, according to which, the destruction mechanism might be inferred preliminarily.

Experimental procedures

Preparation of the bronze

The composition of tin bronze adopted in this work is 89% Cu, 8% Sn and 1% Pb, which is similar to the proportion of unearthed tin bronze in the Shang dynasty, China. The bronze specimens were cut into smaller parts with the dimensions of $10\ mm \times 10\ mm \times 3\ mm$, polished using grit paper gradually to 1000, cleaned ultrasonically with absolute alcohol for 6 min, rinsed with ultrapure water and dried by nitrogen for preparation. Some scholars have researched the patina layer on the surface of bronze cultural relics and found that part of the patina layer contains harmful patinas, part protective patinas. Cu_2O layer, $CuCl$ layer and mixed patina layer were prepared on bronze samples with electrochemical methods. The formation of Cu_2O was performed in a solution consisting of 0.1 mol/L Na_2SO_4 at an anodic potential of 40 mV/SCE [27], while the $CuCl$ patina was synthesized in 0.2 mol/L NH_4Cl

and an anodic current of 5 mA/cm^2 for 20 min [27].The mixed patinated bronze was prepared with the bronze with Cu_2O patina in an aerated solution consisting of 0.028 mol/L NaCl + 0.01 mol/L Na_2SO_4 + 0.016 mol/L $NaHCO_3$ under potential control at + 0.35 V/SCE for 0.5 h and then at + 0.85 V/SCE for 0.5 h [28, 29]. These bronze samples were used for exposure experiments after preparation and will simulate cultural relics to obtain the corrosion behavior of formic acid on them.

Exposure experiment

In order to obtain a certain concentration of formic acid vapor, it can be assumed that the vapor partial pressure of the solvent vapor in the dilute solution is proportional to the mole fraction of the solvent in the solution, which complies with Raoult's law. And it is possible to deduce $G = 0.8\ C/P_0$ through calculating by formula [15], where G is the mass of formic acid in 1000 mL solution, C is the formic acid concentration, and P_0 is the vapor pressure of the pure solvent (formic acid).

Formic acid-contaminated atmospheres were generated by placing an appropriate amount of formic acid solution in the closed reaction vessel, the concentration of the formic acid was 100 ppm, the temperature was controlled around 30 °C, the relative humidity was approximately 100% [14, 15], and the samples were taken out after 4 d, 14 d and 28 d, respectively. The samples before and after exposure were prepared for subsequent analysis.

Analysis methods

Scanning electron microscopy (SEM) was carried out with Hitachi S-3400N to scan the surface topography of the samples before and after exposure experiment. The solid phases formed on the surface of the specimen after exposure were analyzed by X-ray diffraction (D/MAX 2550 VB/PC) and Raman spectroscopy (InVia Reflex), and the corrosion process of the bronze samples in formic acid was further obtained. The X-ray diffraction was equipped with a copper anode X-ray tube and the scan range of diffraction angle $2\theta = 10°–80°$. Raman spectroscopy was performed on the Renishaw's inVia Raman microscope and spectrometer. The bronze samples were irradiated by He–Ne laser at $\lambda = 514.5$ nm, the laser power was 1 mW, and the scanning wavelength was set in the range of 120–4000 cm^{-1}.

Results and discussion

Corrosion products analysis

Figure 1 depicts XRD patterns for specimens exposed to 100 ppm of formic acid vapor for 4, 14 and 28 days. No Sn or Pb compounds were observed in the pattern, which may be due to the low crystallinity or small quantity or the destannification effect. Hence, it mainly considered the conversion and development of copper corrosion products. It could be found from Fig. 1(1) that the peaks of α phase (Cu–Sn)
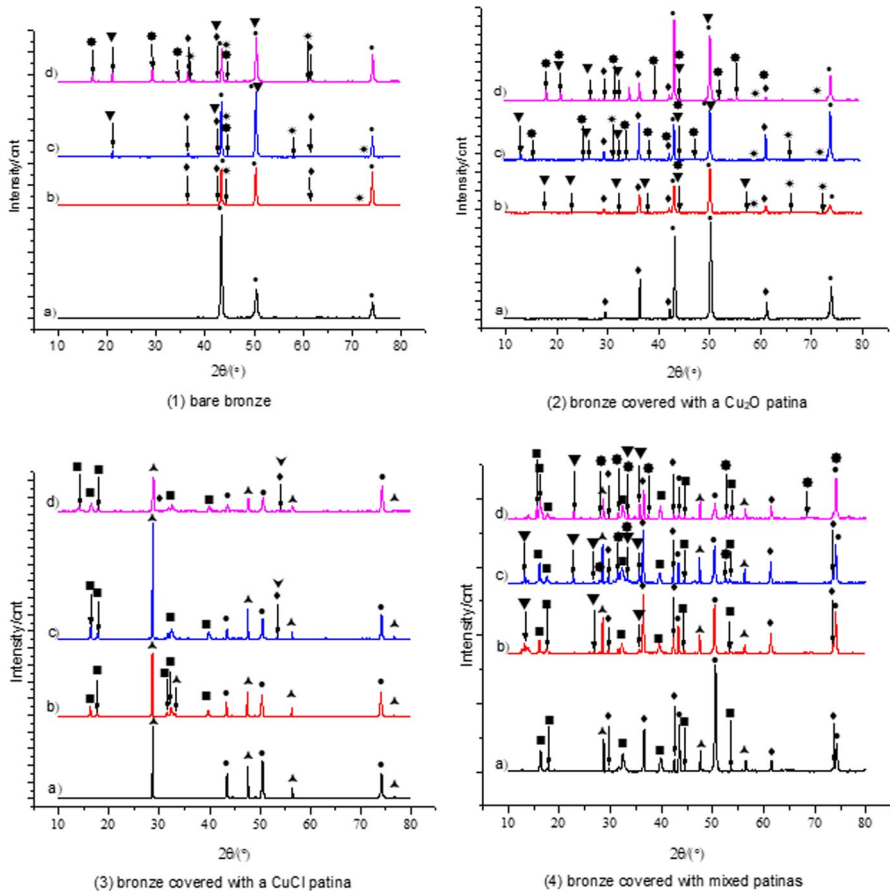
Fig. 1 X-ray diffraction patterns of four kinds of bronze exposed to 100 ppm formic acid at different time: **1** bare bronze, **2** bronze covered with a Cu_2O patina, **3** bronze covered with a CuCl patina and **4** bronze covered with mixed patinas; (a) 0 d, (b) 4 d, (c) 14 d, (d) 28 d, ▼ = Cu(OH)(HCOO); ❀ = $Cu(HCOO)_2$; ▼ = CuO; ✳ = $Cu(OH)_2$; ■ = $Cu_2(OH)_3Cl$; ⊥ = CuCl; ◆ = Cu_2O; ● = Cu–Sn

were observed in the pattern [30, 31]. At the early stage of corrosion, the corrosion products appearing on the surface of the specimen were mainly Cu_2O [32] and a little $Cu(OH)_2$. A small amount of Cu(OH)(HCOO) and $Cu(HCOO)_2$ was generated after 14 days of exposure and more copper formate crystals would be further produced as the exposure time increased to 28 days. It was consistent with the result of SEM analysis of bare bronze (Fig. 2): Before corrosion, the surface of bare bronze had an obvious scratch, then scratches disappeared and the large particles aggregated into sheets, basically covering the bronze surface after 14 days. Figure 1(2) depicts XRD patterns for Cu_2O-covered bronze exposed to the formic acid atmosphere for 4, 14 and 28 days. Only Cu_2O existed on the surface when the sample was exposed to an uncontaminated atmosphere, with the increase in exposure time, $Cu(HCOO)_2$ was generated after the production of $Cu(OH)_2$ and Cu(OH)(HCOO).
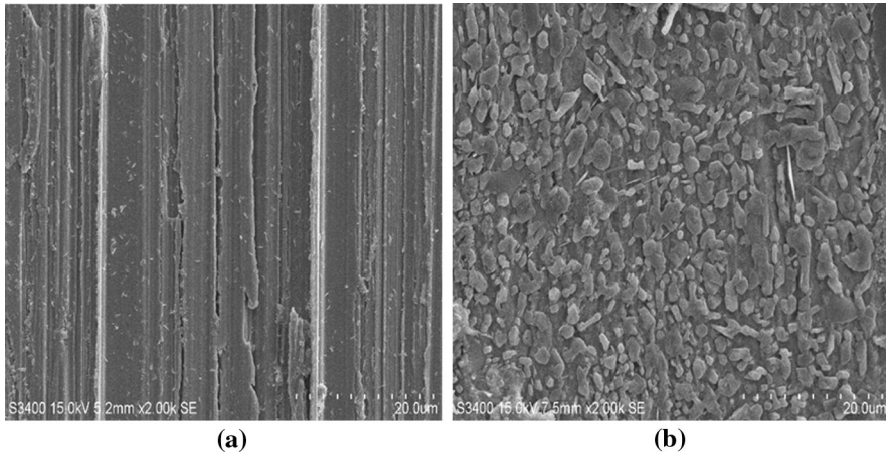
Fig. 2 Surface morphology of bare bronze samples before and after corrosion: **a** 0 d and **b** 14 d

Compared with the early stage of exposure, the amount of Cu(OH)(HCOO) was decreased while the amount of $Cu(HCOO)_2$ was increased. According to the evolution of corrosion product composition over time, the conversion process of Cu_2O-covered bronze was similar to that of bare bronze, except that, the mass of $Cu(HCOO)_2$ and Cu(OH)(HCOO) on the surface of Cu_2O-covered bronze was more than that of bare bronze, indicating that the formic acid-contaminated atmosphere has a strong destructive effect on the Cu_2O patina. And the corrosion may start from attack of the Cu_2O patina, then $Cu(OH)_2$ was gradually transformed into Cu(OH)(HCOO) and further converted into $Cu(HCOO)_2$. It can be confirmed from the SEM micrograph of bronze covered with a Cu_2O patina (Fig. 3): Many fine, compact and
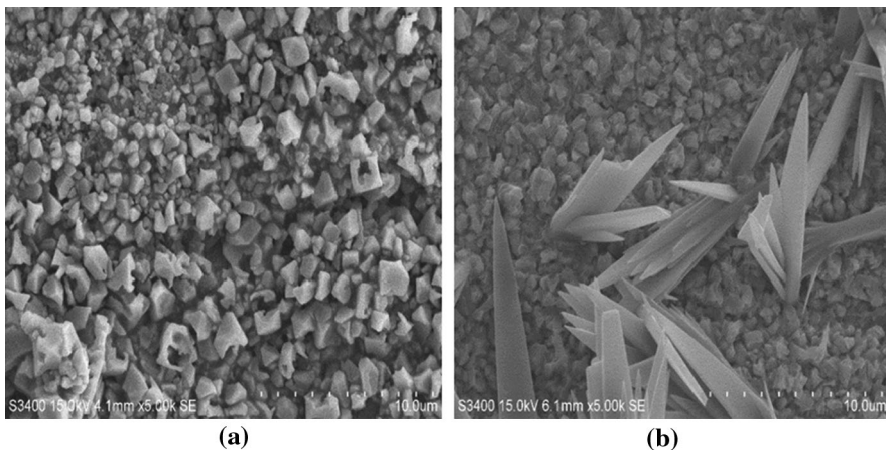

Fig. 3 Surface morphology of Cu_2O-covered bronze before and after corrosion: **a** 0 d and **b** 28 d

uniform cuboidal particles distributed acted as a protective layer on the surface. As the time increased, the corrosion layer appeared to become looser and new long-flaked substances generated on the outer layer which seemed to be poorly adherent $Cu(HCOO)_2$.

Figure 1(3) shows an X-ray diffraction pattern of patinated bronze with CuCl in the formic acid atmosphere for different periods of time. The XRD pattern for the specimen showed the presence of CuCl and α phase (Cu–Sn) before exposure. The SEM micrograph (Fig. 4a) depicted that rough and loose corrosion products appeared on the surface. With the increase in exposure time, $Cu_2(OH)_3Cl$ was further generated. It is easy to find that $Cu_2(OH)_3Cl$ was the main corrosion product, which suggested that CuCl-covered bronze was not directly corroded by formic acid. The formation of $Cu_2(OH)_3Cl$ could be attributed to the reaction between CuCl patina on the sample surface, oxygen and water in a humid environment, which was consistent with the reaction process of powdery rust [33]. According to the surface morphology of bronze covered with a CuCl patina (Fig. 4b), the patina layer on the metal surface seemed very loose and porous, indicating that the substrate could be damaged by the acidic condition. The production of a small amount of Cu_2O and CuO [34] as the exposure time increased to 14 and 28 days confirmed that above. Meanwhile, it was found that $Cu(OH)_2$ and $Cu(HCOO)_2$ would hardly appear in the corrosion product formed on the CuCl-attached bronze, which may suggest that acidic gas might not have time to participate in the reaction during the studied corrosion time.

The qualitative analysis of XRD in Fig. 1(4) revealed that the patina consisted of the following three substances, namely Cu_2O, CuCl and $Cu_2(OH)_3Cl$. Figure 5 shows the surface morphology of bronze with a mixed patina before and after corrosion, demonstrating that the mixed patina was complex and the delamination was obvious, with the increase in exposure time, the type of daisy-like patterns,
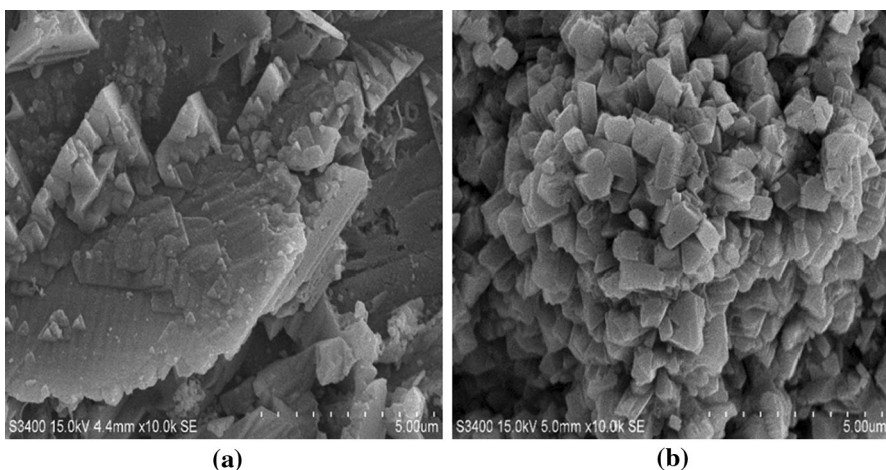

Fig. 4 Surface morphology of bronze covered with a CuCl patina before and after corrosion: **a** 0 d and **b** 14 d
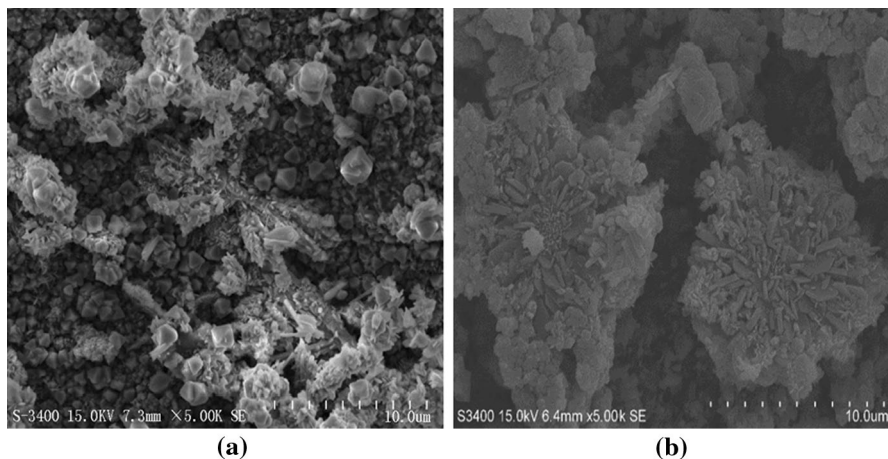
Fig. 5 Surface morphology of bronze covered with mixed patinas before and after corrosion: **a** 0 d and **b** 28 d

converging by long-striped and flaky particles, were generated on the surface. The following compounds produced on the bronze with mixed patinas in the formic acid atmosphere were identified: $Cu(OH)(HCOO)$, $Cu(HCOO)_2$ and $Cu_2(OH)_3Cl$. $Cu_2(OH)_3Cl$ peaks were found in all stages with a slight increase, indicating that $Cu_2(OH)_3Cl$ is relatively stable. $Cu(HCOO)_2$ and $Cu(OH)(HCOO)$ were present in the corrosion products, which illustrated that the reaction of Cu_2O patina and CuCl patina occurred simultaneously.

In order to further validate and analyze the corrosion process, Raman spectra were measured before and after the exposure. The standard characteristic peak positions of the Raman spectra of the copper-containing corrosion products are listed in Table 1, and high-intensity peak positions are underlined [35–40] to facilitate Raman spectroscopic analysis and discussion.

As shown in Fig. 6(1), after 4 days of exposure, the Raman spectrum of bare bronze exhibiting intense peaks at 221 cm^{-1}, 422 cm^{-1} and 644 cm^{-1} is consistent with the standard characteristic peak composition of Cu_2O [36, 40], and these

Table 1 The characteristic peaks of Raman spectra of the corrosion products [35–40]

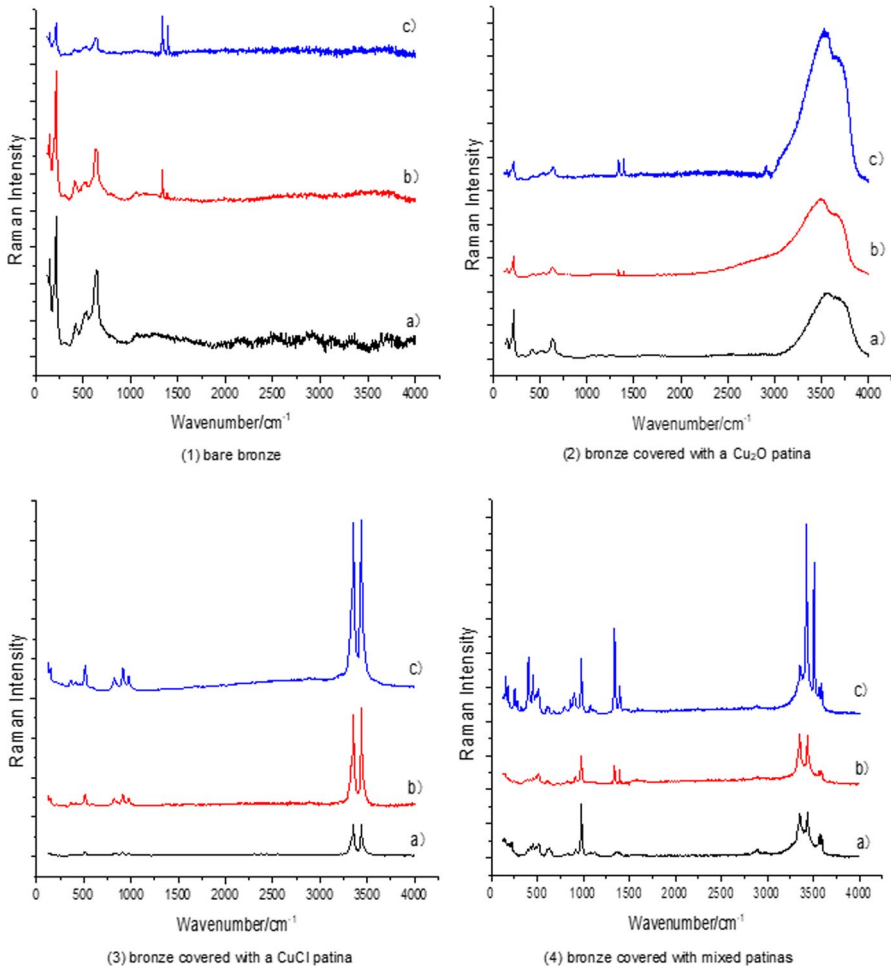| Corrosion products	Position of standard intensity peak (cm^{-1})
CuO	250, 300, 347, 635
Cu_2O	219, 424, 636
CuCl	108, 152, 178, <u>206</u>, 290, <u>463</u>, 613, 1110
$Cu(OH)_2$	292, 470, <u>511</u>, 815, 906, 970
$Cu_2(OH)_3Cl$	149, 360, <u>513</u>, 821, <u>846</u>, <u>911</u>, <u>977</u>, 3314, 3357, <u>3443</u>, <u>3475</u>
$Cu(HCOO)_2$	146, 164, 208, 820, <u>1070</u>, <u>1360</u>, <u>1382</u>, 1550, 2910, 2990

Fig. 6 Raman spectra of four kinds of bronze in 100 ppm formic acid at different time after corrosion: **1** bare bronze **2** bronze covered with a Cu_2O patina **3** bronze covered with a CuCl patina and **4** bronze covered with mixed patinas; (a) 4 d, (b) 14 d, (c) 28 d

intense peaks indicate that some Cu_2O crystals were generated on the bronze surface of at the initial stage of corrosion, whereas the peak at 532 cm^{-1} suggested the presence of copper hydroxide [37, 40]. The peak intensity of Cu_2O and $Cu(OH)_2$ was much weaker when the samples were etched for 14 d, which may be because the generated compounds would further react with formic acid. $Cu(OH)(HCOO)$ seemed to generate from $Cu(OH)_2$, and both phases coexisted in the reaction process [14], which may be the reason for the difficulty measure of $Cu(OH)(HCOO)$. The peaks at 1321 cm^{-1}, 1337 cm^{-1}, 1389 cm^{-1} and 1396 cm^{-1} are consistent with the standard characteristic peaks of $Cu(HCOO)_2$ [39], and the

peak intensity increases with the prolonged time, indicating that $Cu(HCOO)_2$ was generated in the corrosion process.

From Fig. 6(2), the peaks at 218 cm^{-1}, 417 cm^{-1} and 632 cm^{-1} are quite strong and consistent with the characteristic peak of Cu_2O [36, 40]. And the wide and large peak at 3500 cm^{-1} may be the characteristic peak of water molecules and possibly also corresponds to the vibrations of free OH^- [21]. The weak peak at 537 cm^{-1} is close to the characteristic peak of $Cu(OH)_2$ [37, 40], which may be the hydrated form of $Cu(OH)_2$. With the prolongation of exposure time, as shown in (b) and (c), the peaks at 820 cm^{-1}, 1065 cm^{-1} and 1360 cm^{-1} coincide with the standard characteristic peaks of $Cu(HCOO)_2$ [39], suggesting the conversion process from Cu_2O to $Cu(OH)_2$ and finally to $Cu(HCOO)_2$.

Figure 6(3) represents the Raman spectra of the bronze samples covered with CuCl in the formic acid atmosphere. At 363 cm^{-1}, 515 cm^{-1}, 823 cm^{-1}, 911 cm^{-1}, 977 cm^{-1}, 3331 cm^{-1}, 3351 cm^{-1} and 3439 cm^{-1}, the peaks are consistent with the standard characteristic peak of $Cu_2(OH)_3Cl$ [35]. Although the peak intensity is relatively weak, CuCl on the bronze surface quickly reacted with H_2O and O_2 in the air, which had generated $Cu_2(OH)_3Cl$ at the early stage of corrosion. With the prolonged corrosion time, the peak of $Cu_2(OH)_3Cl$ is strengthened, illustrating that the content of $Cu_2(OH)_3Cl$ on the surface of the patinated bronze increased, which was basically consistent with the result of XRD analysis.

The peaks of the bronze covered with mixed patinas in the formic acid atmosphere at 218 cm^{-1} and 451 cm^{-1} correspond with the standard characteristic peaks of Cu_2O [36, 40] after 4 days of exposure. At 218 cm^{-1}, 617 cm^{-1} and 1102 cm^{-1}, the peaks are consistent with the standard characteristic peaks of CuCl [35], and those at 512 cm^{-1}, 911 cm^{-1}, 977 cm^{-1}, 3353 cm^{-1}, 3439 cm^{-1}, 3568 cm^{-1} and 3593 cm^{-1} are in agreement with the standard peaks of $Cu_2(OH)_3Cl$ [35]. These corrosion products have covered on the bronze surface before the exposure experiment. Besides, the peaks at 1373 cm^{-1} and 2889 cm^{-1} correspond with the standard peaks of $Cu(HCOO)_2$ [39], and the peak is weak indicating that a small amount of $Cu(HCOO)_2$ is generated on the samples' surface at the initial stage of corrosion. As shown in (b) and (c) of Fig. 6(4), the peak of basic copper chloride is strengthened, indicating that $Cu_2(OH)_3Cl$ is constantly present in this atmosphere. At 179 cm^{-1}, 1370 cm^{-1}, 1392 cm^{-1}, 1579 cm^{-1} and 2881 cm^{-1}, the peaks are consistent with the standard characteristic peaks of $Cu(HCOO)_2$, and with the exposure to corrosion time, the peaks were significantly enhanced, indicating that more $Cu(HCOO)_2$ was formed. In addition, the corrosion of each patina layer on mixed patinated bronze surface in the formic acid atmosphere was performed at the same time, which was consistent with the XRD analysis and the results.

Possible corrosion mechanism

Although the detailed mechanisms are still unclear, the possible corrosion mechanisms are proposed as follows and schematically displayed in Fig. 7 according to the evolution of corrosion product composition over time:
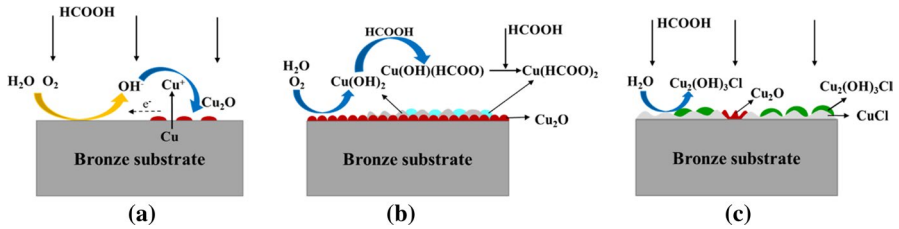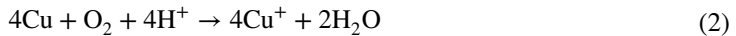
Fig. 7 Possible corrosion mechanisms of patinated bronze in 100 ppm formic acid: **a** bare bronze; **b** Cu$_2$O-covered bronze; **c** CuCl-covered bronze

1. In a humid and weakly acidic environment, the water vapor that is adsorbed on the bronze surface may be catalyzed by formic acid, then Cu is oxidized to copper (I) at the anode, while oxygen is reduced to hydroxyl ions at the cathode, and the generated Cu$^+$ ions could combine with OH$^-$ ions to produce Cu$_2$O [14, 15, 21].

$$O_2 + 2H_2O + 4e^- \rightarrow 4OH^- \tag{1}$$

$$4Cu + O_2 + 4H^+ \rightarrow 4Cu^+ + 2H_2O \tag{2}$$

$$2Cu^+ + 2OH^- \rightarrow Cu_2O + H_2O \tag{3}$$

With the increase in exposure time, Cu$^+$ ions are further oxidized to Cu^{2+}, and Cu^{2+} would react with OH$^-$ ions to produce Cu(OH)$_2$. Cu(OH)(HCOO) and Cu(HCOO)$_2$ are present in the corrosion products because the reaction of Cu(OH)$_2$ in the formic acid-contaminated atmosphere and the corrosion process of Cu$_2$O-covered bronze are similar to that of bare bronze in the formic acid atmosphere. According to the SEM morphology, it is inferred that the attack of Cu$_2$O patina may be the starting point of the corrosion in the presence of formic acid.

$$Cu(OH)_2 + 2HCOOH \rightarrow Cu(HCOO)_2 + 2H_2O \tag{4}$$
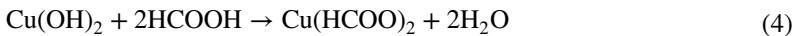
2. In the same exposure environment, Cu$_2$(OH)$_3$Cl is easily generated through reaction between CuCl, water and oxygen in the air [28], indicating that CuCl-covered bronze would not be directly corroded by formic acid. With the prolonged corrosion time, the bronze substrate would be threatened by formic acid due to the loose structure of corrosion products, which can be proved by the appearance of Cu$_2$O and CuO.

$$4CuCl + 4H_2O + O_2 \rightarrow 2Cu_2(OH)_3Cl + 2HCl \tag{5}$$
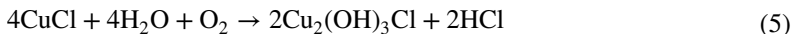
3. For bronze patinated with mixed layers, the corrosion processes of Cu$_2$O patina and CuCl patina occur simultaneously and the products are Cu$_2$(OH)$_3$Cl and Cu(HCOO)$_2$ crystals.

Conclusions

In this study, bare bronze and three types of patina-bearing bronze were investigated in the formic acid-rich environment to reveal the corrosion rules. The formic acid-contaminated atmosphere could not only corrode the bronze substrate, but also destroy the protective Cu_2O patina layer with the formation of $Cu(OH)_2$ which was gradually transformed into $Cu(OH)(HCOO)$ and further converted into $Cu(HCOO)_2$.

Instead of being directly corroded by formic acid, the CuCl patina would react with water and oxygen in the air to produce $Cu_2(OH)_3Cl$. With the increasing exposure time, formic acid would pass through the loose corrosion layer to damage the bronze substrate.

For the bronze covered with mixed patinas, the corrosion process was a combination of bronze covered with Cu_2O patina and that with CuCl patina. In general, it is proved that formic acid has a destructive effect on bronze products, especially artworks and cultural relics.

References

1. C. Zhang, J. Zhao, Res. Chem. Intermed. **44**, 1275 (2018)
2. H.L.Y. Sin, M. Umeda, S. Shironita, A.A. Rahim, B. Saad, Res. Chem. Intermed. **43**, 1919 (2017)
3. J. Huang, X. Meng, Z. Zheng, Y. Gao, Environ. Pollut. **251**, 885 (2019)
4. K. Hachama, A. Khadraoui, M. Zouikri, M. Khodja, A. Khelifa, K. Echiker, B. Hammouti, Res. Chem. Intermed. **42**, 987 (2016)
5. L.T. Gibson, C.M. Watt, Corros. Sci. **52**, 172 (2010)
6. S.D. Zhu, A.Q. Fu, J. Miao, Z.F. Yin, G.S. Zhou, J.F. Wei, Corros. Sci. **53**, 3156 (2011)
7. A. Niklasson, L.G. Johansson, J.E. Svensson, Corros. Sci. **50**, 3031 (2008)
8. A. Kahyarian, A. Schumaker, B. Brown, S. Nesic, Electrochim. Acta **258**, 639 (2017)
9. T. Prosek, M. Taube, F. Dubois, D. Thierry, Corros. Sci. **87**, 376 (2014)
10. P. Qiu, C. Leygraf, J. Electrochem. Soc. **158**, C172 (2011)
11. S.K. Singh, A.K. Mukherjee, M.M. Singh, Indian J. Chem. Technol. **18**, 291 (2011)
12. C. Leygraf, J. Hedberg, P. Qiu, H. Gil, J. Henriquez, C.M. Johnson, Corrosion **63**, 715 (2007)
13. M. Ryhlsvendsen, J. Glastrup, Atmos. Environ. **36**, 3909 (2002)
14. A. Lopez-Delgado, E. Cano, J.M. Bastidas, F.A. Lopez, J. Mater. Sci. **36**, 5203 (2001)
15. E. Cano, C.L. Torres, J.M. Bastidas, Mater. Corros. **52**, 667 (2001)
16. M. Forslund, C. Leygraf, P.M. Claesson, C.J. Lin, J.S. Pan, J. Electrochem. Soc. **160**, C423 (2013)
17. A. Echavarria, A. Rueda, E. Cano, F. Echeverria, C. Arroyave, J.M. Bastidas, J. Electrochem. Soc. **150**, B140 (2003)
18. Y. Jiang, Y. Wu, K. Wang, Mater. Corros. **57**, 418 (2006)
19. A. Niklasson, L.G. Johansson, J.E. Svensson, J. Electrochem. Soc. **154**, C618 (2007)
20. A. Niklasson, L.G. Johansson, J.E. Svensson, J. Electrochem. Soc. **152**, B519 (2005)
21. H. Gil, C. Leygraf, J. Electrochem. Soc. **154**, C611 (2007)
22. M.E. Olvera-Martinez, J. Mendoza-Flores, F.J. Rodriguez-Gomez, R. Duran-Romero, J. Genesca, Mater. Corros. **69**, 376 (2018)
23. P.C. Okafor, B. Brown, S. Nesic, J. Appl. Electrochem. **39**, 873 (2009)
24. K.S. George, S. Nesic, Corrosion **63**, 178 (2007)

25. D.M. Bastidas, M. Criado, S. Fajardo, V.M. La Iglesia, E. Cano, J.M. Bastidas, Int. Mater. Rev. **55**, 99 (2010)
26. T. Kosec, A. Legat, P. Ropret, J. Raman Spectrosc. **45**, 1085 (2014)
27. I. Constantinides, A. Adriaens, F. Adam, Appl. Surf. Sci. **189**, 90 (2002)
28. T. Wang, J. Wang, Y. Wu, Corros. Sci. **97**, 89 (2015)
29. J.M. Bastidas, A. Lopez-Delgado, F.A. Lopez, M.P. Alonso, J. Mater. Sci. **32**, 129 (1997)
30. J. Novakovic, O. Papadopoulou, P. Vassiliou, E. Filippaki, Y. Bassiakos, Anal. Bioanal. Chem. **395**, 2235 (2009)
31. K.M. Zohdy, M.M. Sadawy, M. Ghanem, Mater. Chem. Phys. **147**, 878 (2014)
32. S. Basu, A.K. Sen, Res. Chem. Intermed. **46**, 3545 (2020)
33. C. Fan, C. Wang, S. Wang, Y. Zhang, W. Chase, Z. Han, Sci. China **3**, 239 (1991)
34. W. Li, Y. Wu, Y. Gao, S. Xing, Res. Chem. Intermed. **45**, 5549 (2019)
35. R.L. Frost, Spectrochim. Acta A **59**, 1195 (2003)
36. X. Zhang, I.O. Wallinder, C. Leygraf, Corros. Sci. **85**, 15 (2014)
37. R.L. Frost, P.A. Williams, J.T. Kloprogge, W. Martens, Neues Jahrbuch für Mineralogie Monatshefte **10**, 433 (2003)
38. M. Pohl, C. Hanewinkel, A. Otto, J. Raman Spectrosc. **27**, 805 (1996)
39. J. Berger, J. Phys. C Solid State Phys. **8**, 2903 (1975)
40. J.C. Hamilton, J.C. Farmer, R.J. Anderson, J. Electrochem. Soc. **133**, 739 (1986)